Rev.Adv.Mater.Sci. 15(2007) 33-37

Zr-Al-N NANOCOMPOSITE COATINGS DEPOSITED BY PULSE MAGNETRON SPUTTERING

H. Klostermann, F. Fietzke, T. Modes and O. Zywitzki

Fraunhofer Institut für Elektronenstrahl- und Plasmatechnik (FEP), Winterbergstrasse 28, 01277 Dresden, Germany

Received: January 22, 2007

Abstract. $Zr_{1-x}Al_xN$ layers have been deposited in the full compositional range (x = 0…1) by adjusting working point and pulse times for reactive pulsed magnetron co-sputtering of aluminium and zirconium targets. Whereas ZrN is known to be a hard coating material with properties similar to the well established TiN, yet a higher oxidation resistance, no enhanced hardness is found for $Zr_{1-x}Al_xN$ in a range x=0.3…0.9, as it is the case for $Ti_{1-x}Al_xN$ with x = 0.5…0.7. However, films with a fraction of only a few atomic percent aluminium exhibit enhanced hardness up to 30 GPa, which is well above the hardness of pure ZrN or pure AlN (25 GPa both) deposited by reactive pulse magnetron sputtering.

XRD investigations reveal the nanocrystalline nature of the coating with a grain size of 10 nm for the cubic structure ZrN with a (100) preferred orientation. It is believed that Al acts as an impurity which limits the grain growth and initiates frequent re-nucleation of ZrN-crystallites. Thereby, the nanocrystalline structure is formed with a maximum in hardness for an optimum Al concentration of approximately 5 at.%.

1. INTRODUCTION

Besides the design of multilayer systems to increase the performance of functional coatings, the search for sophisticated layer materials determines the advances in coating development. Following basic research on superlattices that show extraordinary structural and mechanical behaviour due to their nanometer scale phase alternation in growth direction, it has been attempted to exploit such structures for application in the field of wear resistance. This route has been pursued successfully with a number of material systems, among them Ti-Al-N [1], Ti-(Al-)Me-N (Me∈{Cr, Zr, Nb, Y, V}) [2,3], and CrN-NbN [4], to mention only the most important. It has also been found that a hardening effect due to nanoscale phase separation can also arise in three dimensions, when nanocomposite structures form [5,6]. Superhard nanocomposites are mainly composed of two phases, which are at least partially immiscible. The theoretical model of nanocomposites is that the predominant phase is nanocrystalline and is surrounded by a second minor phase, which is segregated in a monolayer on the grain boundaries. It is supposed that this special nanocomposite structure is formed by spinodal decomposition. The second minor phase should prevent the sliding of grain boundaries [7]. Again, material systems including TiAlN as one phase and one or more of {Si, C, B, W, Mo} have been investigated and, according to their performance, are considered as cutting-edge wear resistant coatings [8,9]. $Ti_{1-x}Al_xN$ itself forms a

Corresponding author: H. Klostermann, e-mail: heidrun.klostermann@fep.fraunhofer.de

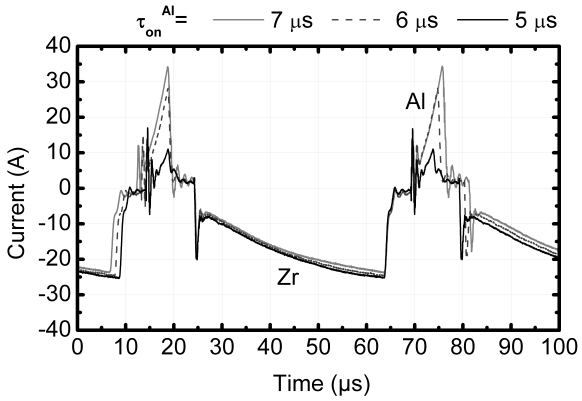

Fig. 1. Temporal evolution of discharge current in the bipolar reactive Zr-Al co-sputtering process in Ar-N_2 gas mixture. Represented are three different pulse lengths of the Al-sputtering pulse resulting in small Al-fractions.

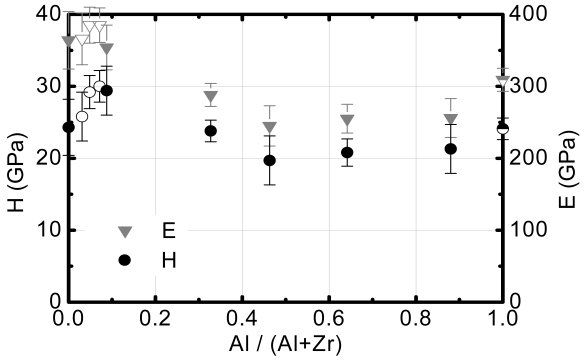

Fig. 2. Dependence of hardness and Youngs modulus on the metal composition of $Zr_{1-x}Al_xN$ films. All films are approximately stoichiometric (N:Me=0.9…1). Open/filled symbols denote films from different experimental series.

nanocomposite structure of nanocrystalline (nc) cubic rock salt structure (Ti,Al)N and hexagonal wurtzite structure AlN in the compositional range x=0.5…0.7, which is due to the segregation of AlN once the solubility threshold of Al in (Ti,Al)N is reached or surpassed ($x \geq 0.52$) [10]. This nc-(Ti,Al)N/nc-AlN structure has been produced by reactive magnetron co-sputtering of Ti and Al on stationary substrates [10] as well as in production scale equipment on moving substrates [11], where, in addition, a nanometer scale multilayer sequence arises from dynamic deposition [12]. In the latter work, bipolar pulsed sputtering allowed fine scanning of the composition through variation of pulse lengths. With optimised deposition parameters, these coatings reach hardness up to 38 GPa and good thermal oxidation resistance up to 800 °C [12].

Although, from a theoretical point of view, the system Zr-Al-N too has the possibility to form single-phase solid solution and two-phase composite structures [13], there is less evidence for a correspondingly increased performance of ZrAlN as for TiAlN [14].

By scanning the compositional range of $Zr_{1-x}Al_xN$ from x=0 to x=1, we have investigated whether a two phase structure with increased hardness with respect to standard ZrN coatings can be found. The perspective would be an even increased oxidation resistance of such a coating due to the intrinsically higher oxidation resistance of ZrN with respect to TiN in combination with the formation of a protective Al_2O_3 top layer as known from the system Ti-Al-N.

2. EXPERIMENTAL

Layers are deposited by reactive pulse magnetron sputtering from a dual magnetron system (DMS) with target size of 500×120 mm in a production scale batch coating device of volume 1 m^3. A rotary substrate holder enables one-, two- or three-fold rotation of the substrates for coating of components. For substrate heating a heater is located in the centre of the vacuum chamber, such that substrates can rotate between the heater and the DMS.

The recipient is evacuated down to a base pressure of 10^{-3} Pa. The DMS is powered by a pulse voltage supply (MAGPULS Q-1000/60/500 BP) with a frequency in the range 16…25 kHz in bipolar mode. An additional pulse power supply is available for plasma pre-treatment and substrate biasing. For tuning of the Zr/Al ratio, the DMS is equipped with pure aluminum (99.99%) and zirconium (99.2%) targets, which are co-sputtered in an argon-nitrogen atmosphere using a working pressure of 0.45 Pa. Polished steel substrates of hardened ball bearing steel (100Cr6) are coated while they perform a one-fold rotation in front of the DMS. Layers with a thickness between 2.0 and 4.7 µm are deposited at deposition rates between 60 and 80 nm/min. The substrate temperature during deposition of the layers is between 350 °C and 400 °C. A negative dc bias voltage of 50 V is applied to the substrates.

Hardness and Youngs modulus of the films are determined by nanoindentation technique (MTS, Nano-Indenter XP) using continuous stiffness mea-

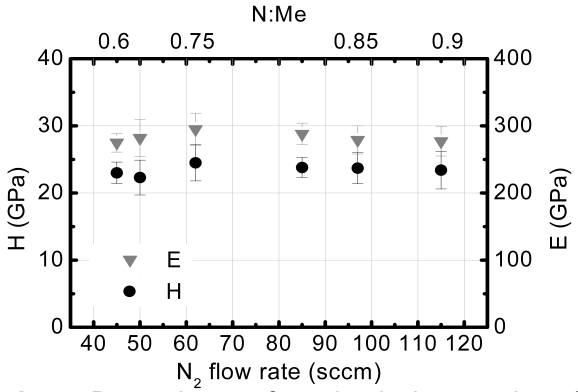

Fig. 3. Dependence of mechanical properties of films on the nitrogen content of the working gas (fixed argon flow rate of 300 sccm). The stoichiometry (N:Me) of the films ranges from 0.6 to 0.9 (see top axis).The metal ratio of the films is constant Al:Zr=0.41±0.05, or *x*=0.3±0.03. The mechanical properties are nearly constant.

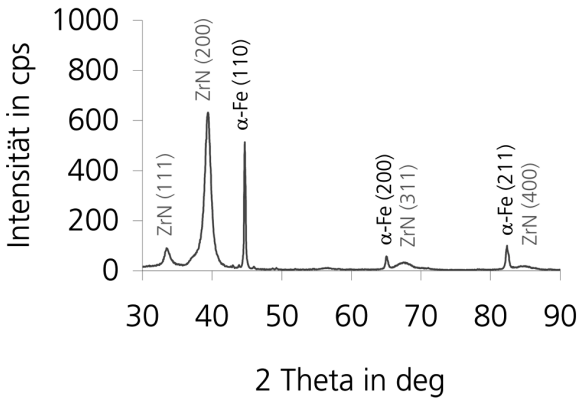

Fig. 4. Diffraction pattern of a $Zr_{1-x}Al_xN$ with x=0.05 exhibiting increased hardness of 29 GPa. Only cubic structure ZrN with a grain size of 10 nm (FWHM) can be identified in the pattern.

surement and Oliver and Pharr theory for evaluation [15]. The chemical composition of the films has been determined by energy dispersive spectroscopy and/or by glow discharge optical emission spectrometry depth profiling (GD-OES; Leco, GDS-750). Film structure has been investigated by X-ray diffraction using Cu-K_α radiation (XRD; Bruker-AXS D8).

3. RESULTS AND DISCUSSION

Pulse magnetron sputtering in bipolar mode is known to imply high energy of the charge carriers in the plasma. This fact makes it especially suitable for the deposition of hard, protective coatings, where a dense morphology, good scratch resistance and a high hardness are crucial for the function of the coating. Optimization of the coating composition is a complementary task. Bipolar pulsed sputtering offers the possibility of finely tuning the composition of layers by adjusting the pulse lengths for two targets of different material sputtered in a dual magnetron system. Fig. 1 illustrates this in three different time series of the discharge current with slightly changed pulse durations of the Al-sputtering pulse at constant Zr sputtering pulse duration and constant off-times. A bipolar voltage of 900 V is applied between the targets. The difference in chemical reactivity of the two materials and in the characteristic properties of the reaction products on the two targets lead to distinct impedances in the respective sputter phases. The current increase is much steeper in the Al-sputtering phase than in the Zr-sputtering phase. Correspondingly, at equal pulse durations, the pulse amplitude is much higher in the Al-sputtering phase than in the Zr-sputtering phase.

Changing the pulse durations of the sputter pulses, we have scanned the compositional range of $Zr_{1-x}Al_xN$ films from *x*=0 to *x*=1, looking for compositions that provoke an enhancement of mechanical properties. The result is shown in Fig. 2, where hardness and Youngs modulus of the layers is plotted as a function of the Al-fraction in the metal component. All coatings are nearly stoichiometric with a ratio N:Me = 0.9…1 determined by EDX and/or GDOES.

For most compositions, hardness lies in the range of 20…24 GPa, also for pure ZrN or pure AlN coatings. ZrN has, however, a higher Youngs modulus of 360 GPa against 310 GPa of pure AlN films and values around 250 GPa for mixed phase films.

A significant increase in hardness is found for small Al-fractions of 3…5%. A singular value in a first deposition series has been confirmed by a second series (open symbols in Fig. 2) with a finer scanning of the range *x*=0…0.05. Hardness increases by 25% with respect to ZrN and reaches values of 30 GPa, whereas Youngs modulus increases only moderately. This is an indication that the fundamental crystal lattice structure is not changed.

Indeed, XRD investigation of the films with increased hardness reveal a cubic structure ZrN with

a very small grain size of 10 nm, which has been estimated from the FWHM using the Scherrer formula. The diffraction pattern is shown in Fig. 4. The ZrN displays a pronounced (100) preferential orientation.

All films in the range x=0.3…0.9 exhibit approximately the same mechanical properties, although their visual appearance ranges from violet (x=0.3) over dark grey (x=0.7) to mostly transparent (x=0.9). Pure ZrN films are of golden color, pure AlN films are highly transparent.

We further attempted to produce films of different stoichiometry N:Me by changing the amount of reactive gas (nitrogen) at constant argon flow rate. It turned out that, for fixed pulse durations, the change in reactivity does not significantly alter the metal composition in the film. Nor does it influence the mechanical properties, which can be seen in Fig. 3. For a $Zr_{0.7}Al_{0.3}N$ film (x=0.30±0.03), hardness remains constant at 23 GPa and Youngs modulus at 280 GPa to within 5%, in a range of stoichiometry from N:Me=0.6 to N:Me=0.9 (top axis in Fig. 3). Again, there is a color change from metallic-gold for the film with lowest nitrogen content to dark bronze-violet for the film with highest nitrogen content.

Our results are in contrast to recent work on the $Zr_{1-x}Al_xN$ thin films, where a hardness increase from 21 GPa to 28 GPa has been detected as the Al-content in the films increased from x=0.1 to x=0.43 [14]. However, in the range of small Al-contents, they correspond to previous work on nc-ZrN/Me nanocomposite structures with Me ∈ {Cu, Ni, Y}, where similar results have been obtained [16-19]. Considering these as well as our findings, the action of the small amount of Al is believed to play the role of a grain refining impurity in ZrN crystalline film growth [20].

4. SUMMARY

The structure and nanomechanical properties of the system $Zr_{1-x}Al_xN$ has been investigated by scanning the full compositional range from x=0 to x=1. Films have been deposited by bipolar pulse magnetron sputtering in production scale equipment on moving substrates by co-sputtering a zirconium and an aluminium target in argon-nitrogen gas mixtures. The composition can be finely adjusted by varying the pulse lengths of the sputter pulses in bipolar MF-pulse sputtering. A significant increase in hardness, from 24 GPa to 30 GPa, has been detected for films with only a small fraction of 3…5% Al in the metal component. It is believed, that Al in this case acts as an impurity that inhibits grain growth and initiates frequent re-nucleation of ZrN crystallites. Grain size is calculated from the FWHM of X-ray diffraction peaks and is found to be approximately 10 nm. Similar results have been obtained for nc-ZrN/Me nanocomposite structures with Me ∈ {Cu, Ni, Y} for small concentrations of Me [16-19].

In contrast to the system Ti-Al-N, no two-phase nanocomposite structure of the type nc-ZrAlN/nc-AlN could be produced that exhibited enhanced hardness due to the specific nanocomposite structure including two distinct crystalline phases. This result can probably be related to the finding that, contrary to TiN-AlN, in ZrN-AlN superlattices the cubic phase AlN can not be stabilized, supposedly due to a larger lattice mismatch between ZrN and AlN [21]. Cubic structure AlN is suspected to play a crucial role also in spinodal decomposition of (Ti,Al)N beyond the solubility threshold of Al.

REFERENCES

[1] Y.Y. Wang, M.S. Wong, W.J. Chia, J. Rechner and W.D. Sproul // *J. Vac. Sci. Technol. A* **16** (1998) 3341.
[2] O. Knotek, M. Böhmer and T. Leyendecker // *J. Vac. Sci. Technol. A* **4** (1986) 2695.
[3] W.D. Sproul // *Science* **273** (1996) 889.
[4] P.Eh. Hovsepian, D.B. Lewis and W.-D. Münz // *Surf. Coat. Technol.* **133-134** (2000) 166.
[5] S. Veprek // *J. Vac. Sci. Technol. A* **17**(5) (1999) 2401.
[6] J. Musil // *Surf. Coat. Technol.* **125** (2000) 322.
[7] S. Veprek, M. G. J. Veprek-Heijman, P. Karvankova and J. Prochazka // *Thin Solid Films* **476** (2005) 1.
[8] P. Holubar, M. Jilek and M. Sima // *Surf. Coat. Technol.* **133-134** (2000) 145.
[9] J. Patscheider, T. Zehnder and M. Disserens // *Surf. Coat. Technol.* **146-147** (2001) 201.
[10] J. Musil and H. Hruby // *Thin Solid Films* **365** (2000) 104.
[11] H. Klostermann, B. Böcher, F. Fietzke, T. Modes and O. Zywitzki // *Surf. Coat. Technol.* **200** (2005) 760.
[12] O. Zywitzki, H. Klostermann, F. Fietzke and T. Modes // *Surf. Coat. Technol.* **200** (2006) 6522.
[13] H. Holleck // *Surf. Coat. Technol.* **36** (1988) 151.

[14] R. Sanjínes, C.S. Sandu, R. Lamni and F. Lévy // *Surf. Coat. Technol.* **200** (2006) 6308.
[15] W. C. Oliver and G. M. Pharr // *J. Mater. Res.* **7** (1992) 1564.
[16] J. Musil, P. Zeman, H. Hrubý and P.H. Mayrhofer // *Surf. Coat. Technol.* **120-121** (1999) 179.
[17] J. Musil, J. Vlček, P. Zeman, Y. Setsuhara, S. Miyake, S. Konuma, M. Kumagai and C. Mitterer // *Jpn. J. Appl.Phys.* **41** (2002) 6529.
[18] J. Musil, P. Karvánková and J. Kasl // *Surf. Coat. Technol.* **139** (2001) 101.
[19] J. Musil and P. Poláková // *Surf. Coat. Technol.* **127** (2000) 99.
[20] P.B. Barna and M. Adamik // *Thin Solid Films* **317** (1998) 27.
[21] M.-S. Wong, G.-Y. Hsiao and S.-Y. Yang // *Surf. Coat. Technol.* **133-134** (2000) 160.